Control of Spatiotemporal Coherence of a Thalamic Oscillation by Corticothalamic Feedback

Diego Contreras, Alain Destexhe, Terrence J. Sejnowski, Mircea Steriade*

The mammalian thalamus is the gateway to the cortex for most sensory modalities. Nearly all thalamic nuclei also receive massive feedback projections from the cortical region to which they project. In this study, the spatiotemporal properties of synchronized thalamic spindle oscillations (7 to 14 hertz) were investigated in barbiturate-anesthetized cats, before and after removal of the cortex. After complete ipsilateral decortication, the long-range synchronization of thalamic spindles in the intact cortex hemisphere changed into disorganized patterns with low spatiotemporal coherence. Local thalamic synchrony was still present, as demonstrated by dual intracellular recordings from nearby neurons. In the cortex, synchrony was insensitive to the disruption of horizontal intracortical connections. These results indicate that the global coherence of thalamic oscillations is determined by corticothalamic projections.

Despite the pervasive presence of corticothalamic rhythms during sleep, their function remains a mystery. Recently, the mechanisms underlying the generation of sleep spindles have been elucidated (*1*). Spindles are sequences of waxing and waning field-potential oscillations at 7 to 14 Hz, lasting for 1 to 3 s and recurring every 3 to 10 s. The spindles represent an electrographic landmark of light sleep and are associated with loss of perceptual awareness. Spindle oscillations are present in the thalamus after removal of the cerebral cortex (*2*), but are less well organized, as we demonstrate here.

Participation of the corticothalamic projection in the generation of spindles was first proposed by Morison and Dempsey (*3*), on the basis of potentiation of thalamic spindles by cortical application of acetylcholine. Others have disagreed (*4*), but more recent experiments have shown that the threshold for evoking spindles is lower for corticothalamic than for prethalamic stimulation and that cortical stimulation increases the synchrony of spindling among couples of thalamic cells (*5*). Moreover, the spontaneous slow sleep oscillation is associated with a corticothalamic drive that triggers a brief sequence of spindle waves (*6*).

Most of the hypotheses regarding the function of the corticothalamic projection are related to information processing in the awake state. It was proposed that *N*-methyl-D-aspartate receptor activation in thalamocortical (TC) cells by cortical afferents increases the gain of the TC path only if TC cells are already depolarized by prethalamic inputs (*7*). Recently, a specific role for the feedback projections from the visual cortex to the lateral geniculate (LG) nucleus was suggested, on the basis of the observation that LG cells showed stimulus-dependent synchronization, which was disrupted by removal of the visual cortex (*8*). This observation indicates a dynamic role for the corticothalamic feedback projection in selecting or focusing input signals with specific features. The corticothalamic feedback may also be an essential component in shaping dynamic spatiotemporal maps that code for stimulus information in the somatosensory thalamus (*9*).

We investigated the influence of the massive corticothalamic projection on the spatiotemporal coherence of spontaneously occurring global spindle oscillations generated in the cat thalamus under barbiturate anesthesia. Recording of local field potentials (LFPs) from the thalamus, with eight tungsten electrodes (Fig. 1) designated Th1 through Th8, revealed that spindling occurs almost simultaneously in most of the thalamus (Fig. 1, Intact). Recordings with the cortex intact (Fig. 1) showed that spindling in the thalamus tended to start and finish within narrow time windows in all eight electrodes. Variations of the initiation and

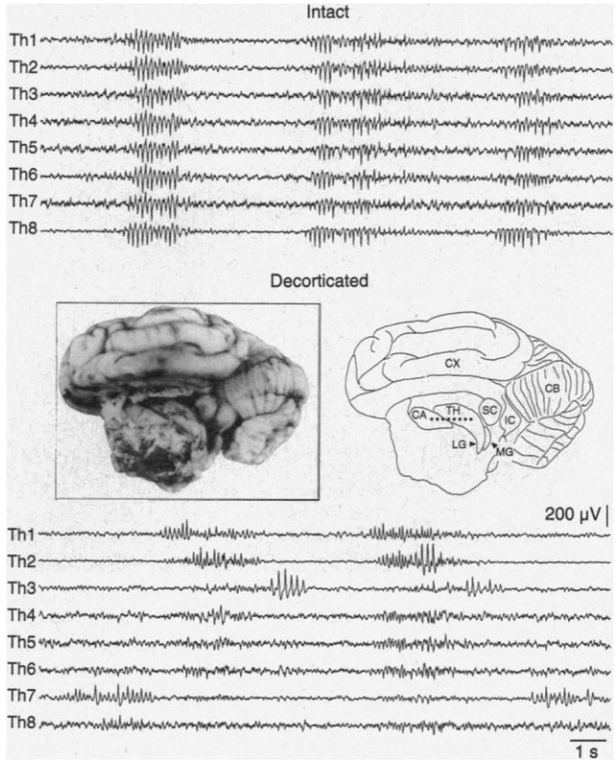

Fig. 1. Effect of removal of the cerebral cortex on the pattern of generation of spindle oscillations in the thalamus. In an intact thalamocortical network under barbiturate anesthesia (upper panel), three spontaneous spindle sequences at 8 to 9 Hz and lasting for 1 to 3 s occurred at roughly the same time in the LFPs recorded from eight tungsten electrodes (Th1 through Th8). Tip resistances were 1 to 5 megohms, and interelectrode distances were 1 mm. Negativity downward. Cortex was removed by suction after careful cauterization with silver nitrate (photo), exposing the head of the caudate nucleus (CA), most of the dorsal thalamus (TH), the lateral geniculate body (LG), the medial geniculate body (MG), and the superior and inferior colliculi (SC and IC). Also in the photo, and represented in the drawing at right, are the intact contralateral cortex (CX) and the cerebellum (CB). The eight electrodes were held together and descended at the positions indicated (black dots) in the drawing. The two or three most anterior electrodes crossed through the head of the CA to reach the thalamus. After decortication (lower panel), recordings from approximately the same thalamic locations showed that spindling continued to occur at each electrode site, but their coincidence in time was largely diminished. The eight-electrode configuration was positioned in different cats at various depths within the thalamus (from stereotaxic coordinates 2 to 6) and different lateral planes (from 2 to 5); all positions essentially gave the same result.

D. Contreras, A. Destexhe, M. Steriade, Laboratoire de Neurophysiologie, Faculté de Médecine, Université Laval, Quebec G1K 7P4, Canada.
T. J. Sejnowski, Howard Hughes Medical Institute, The Salk Institute for Biological Studies, 10010 North Torrey Pines Road, La Jolla, CA 92037, and Department of Biology, University of California San Diego, La Jolla, CA 92093, USA.
*To whom correspondence should be addressed.

termination time of spindle sequences were less than 10% of the duration of a spindle sequence. We then removed the cortex by suction (n = 8) and replaced the electrodes in approximately the same position (Fig. 1). In the decorticated cat, the occurrence of spindle sequences in the different electrodes was largely not coincident in time (*10*); however, some spindle sequences were still nearly synchronous (Fig. 1, Decorticated).

To compare the spatiotemporal characteristics of spindle oscillations in the thalamus before and after decortication, we constructed spatiotemporal maps of activity (Fig. 2, top) by plotting the LFP voltage as a function of time and space. In the left panel, with intact cortex, oscillatory activity was highly coherent over the entire recorded thalamic area, as indicated by the formation of horizontal yellow (maximum local activity) and blue (local silence) stripes at 8 to 10 Hz on the vertical columns. Not only were spindle sequences initiated synchronously, but each oscillatory cycle formed uninterrupted yellow and blue stripes across the thalamic activity maps. These stripes were not perfectly horizontal, which indicates the existence of phase shifts among the thalamic sites. Removal of the cortex markedly diminished the spatiotemporal coherence, as shown by the disorganized pattern (Fig. 2, Decorticated) with an absence of stripes, indicating that oscillatory activity was no longer synchronized among thalamic sites located more than 2 or 3 mm apart.

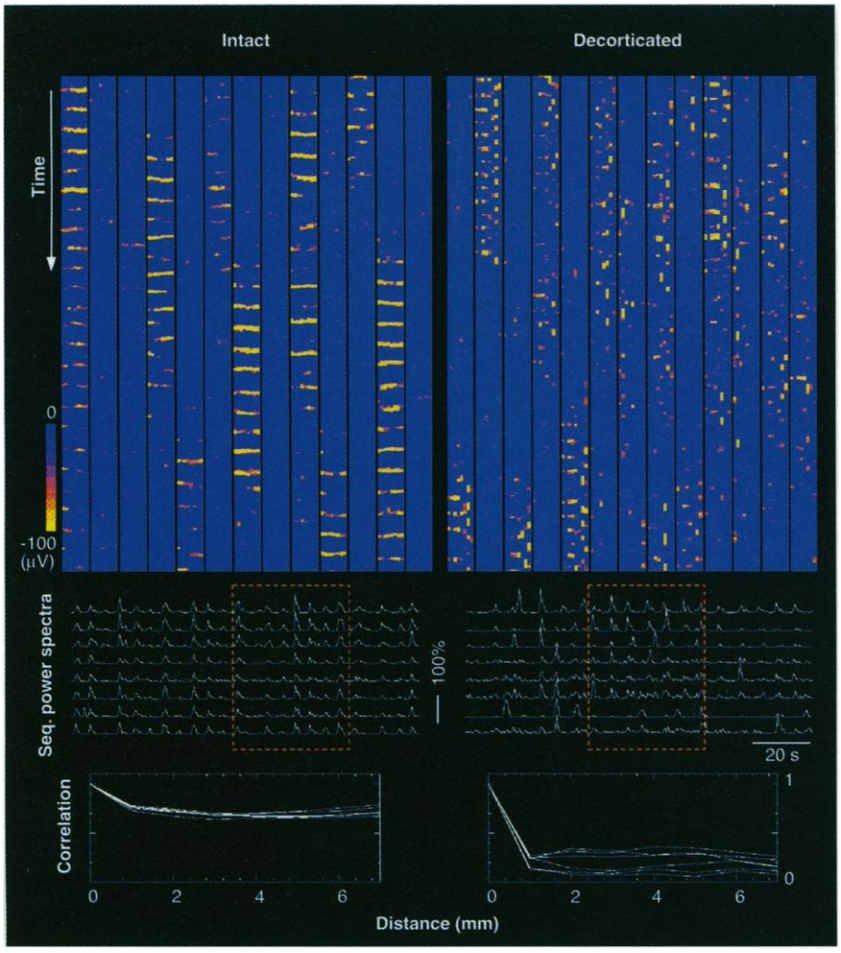

Fig. 2. Disruption of the spatiotemporal coherence of thalamic oscillations after removal of the cortex. (**Top**) Spatiotemporal maps of electrical activity across the thalamus were constructed by plotting time (time runs from top to bottom in each column; arrow indicates 1 s), space (from left to right, the width of each column represents 8 mm in the anteroposterior axis of the thalamus), and LFP voltage [from blue to yellow, color represents the amplitude of the negative deflections of thalamic LFPs; the color scale ranged in 10 steps from the baseline (blue) to −100 μV (yellow)]. Time was divided into frames, each representing a snapshot of 4 ms of thalamic activity. A total of 40 s is represented (9880 frames). Each frame consisted of eight color spots, each corresponding to the LFP of one electrode from anterior to posterior (left to right in each column). (**Middle**) Sequential power spectra were evaluated at each site for a 0.5-s window. The total power of the 7- to 14-Hz frequency band, normalized to the 100% of the highest peak obtained, was represented as a function of time (dashed box in red indicates the 40 s shown in top panels). (**Bottom**) Decay of correlation with distance. Crosscorrelations were computed for all possible pairs of sites, and the value at time zero from each correlation was represented as a function of the intersite distance for six different consecutive epochs of 20 s. Spatial correlation was calculated for thalamic recordings in the intact brain (left) and after removal of the cortex (right).

The coincidence in the appearance of spindle oscillations among the eight electrodes was analyzed by calculating the sequential power spectra (Fig. 2) (*11*). The total power of spindling frequency increased and decreased coherently among the eight electrodes in the intact-cortex condition (Fig. 2, left). After decortication, oscillatory activity no longer appeared in a concerted manner among the electrodes.

To quantify the effect of cortex removal on thalamic synchronization, we calculated the decay of correlation with distance (Fig. 2, bottom), for distances of 0 to 7 mm in steps of 1 mm, as determined by the configuration of the recording electrodes. In the intact cortex hemisphere, correlations showed a limited decay with distance, with values around 0.7 (0.72 ± 0.06, mean ± SE, n = 8) for distances up to 7 mm. After decortication, spatial correlation decreased stepwise to values around 0.2 to 0.3 (0.21 ± 0.11, n = 8) for distances greater than 1 mm.

The presence of spindle oscillations in the LFPs after decortication indicates that local synchrony is still maintained by intrathalamic connectivity. This effect can be determined by the pattern of divergent connections between thalamic reticular (RE) and TC cells (*12*). To demonstrate local synchrony after decortication, we performed dual intracellular recordings (*13*) of pairs of TC cells in the decorticated thalamus at short and long interelectrode distances (Fig. 3). Intracellular recordings from TC cells revealed the typical pattern of spindle-related events (*14*). Pairs of cells at a 1-mm distance, recorded from the ventrolateral (VL) nucleus (Fig. 3A), showed spontaneous spindle sequences that were nearly synchronous between the two TC cells (Fig. 3A, cells designated TC1 and TC2). When the cells were recorded from the VL and the lateral posterior (LP) nucleus, at ~4 mm distance in the anteroposterior axis, spontaneous spindle sequences from both cells were no longer coincident in time, and the superposition of spindle-related inhibitory postsynaptic potentials (IPSPs) in one cell gave rise to a flat line in the other cell (Fig. 3B). Thus, closely located cells within the VL nucleus showed almost simultaneous IPSPs, indicating that they were produced by a pool of synchronized RE cells (*15*), whereas more distant cells generally showed no consistent rela-

tion between their spindle-related intracellular activities.

A possible mechanism by which the cortex exerts its global effect on spatiotemporal organization of thalamic oscillations is the more divergent projection of corticothalamic axons as compared to the reciprocal projections between the RE nucleus and the dorsal thalamus. The action of the cortex could be exerted through direct excitation of TC cells, timing their output spike-bursts by precipitating the offset of the cyclic IPSPs; through excitation of RE cells and synchronization of the onset of the IPSPs; or both. We favor the role of the RE nucleus, taking into consideration the divergent projections of its rostral pole (*14*), that in turn receives convergent projections from various cortical areas (*12*).

An alternative explanation for the synchronizing role of the cortex would be that synchrony is attained within cortical circuits because of the abundant horizontal corticocortical projections in areas 5 through 7 (*16*) and thereafter is imposed on the thalamus. To investigate the role of intracortical connectivity on synchrony, we performed multisite recordings from the suprasylvian cortex, using the same array of electrodes as for thalamic recordings. In control conditions (Fig. 4A, Intact), spontaneous spindle oscillations occurred at 8 to 9 Hz almost simultaneously in the eight leads, reflecting the synchrony recorded in the thalamus with intact cortex (Fig. 1). After a deep coronal cut through the suprasylvian gyrus (Fig. 4A, Cut), cortex leads Cx4 and Cx5 showed diminished activity due to local damage, but spontaneous oscillations still occurred simultaneously in the other leads. To quantify the effect of disruption of intracortical connections, we calculated the averaged crosscorrelations between sites separated by increasing distances (Fig. 4B). Similar to thalamic recordings (Fig. 2), correlations showed a smooth decay with increased distance in the cortex. After the cut, a gap appeared in correlations 1-4 and 1-5 due to tissue damage, but the same correlation patterns were seen at distances of 5 mm and greater (*17*).

These results are consistent with a decisive role for corticothalamic projections in organizing the long-range synchrony and spatiotemporal patterns of oscillations generated in the thalamus. The natural consequence of thalamic synchrony is that the impact of thalamic output to the cortex is increased during this sleep oscillation. Whether this represents a mere consequence of the type of connectivity between cortex and thalamus subserving information processing or has in itself a precise physiological role is a question whose answer is still far from our reach.

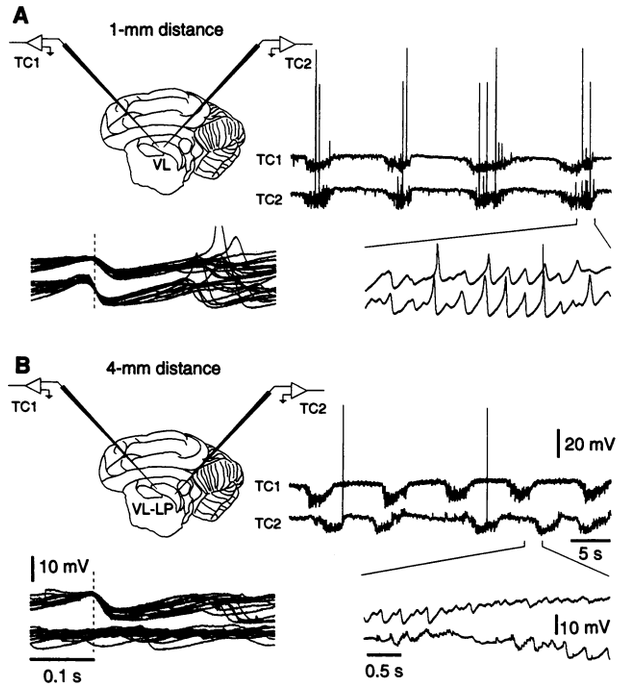

Fig. 3. Synchronized spindle sequences of closely located TC cells in the decorticated thalamus. (**A**) Couples of TC cells (designated TC1 and TC2) were intracellularly recorded at distances around or less than 1 mm (n = 5) from the VL nucleus. Spindle sequences occurred at the same time in both cells (spontaneous activity at right). The rightmost sequence expanded below shows the synchrony of the intracellular events characteristic of spindling. Spindling-related IPSPs (n = 10) from TC1 were aligned, with the time of their onset as a zero time reference (dotted line). The intracellular recording from TC2 was aligned to the same reference, revealing the occurrence of IPSPs that were almost simultaneous with TC1. (**B**) TC cells were recorded simultaneously from the VL nucleus (TC1) and the LP nucleus (TC2), distant by 4 mm. Spindles occurring spontaneously in each cell showed no consistent temporal relation. The spindling sequence expanded below shows that the termination of a spindle in TC1 coincides with the beginning of a spindle in TC2. Alignment of IPSPs (n = 10) from TC1 compared with a flat line in TC2.

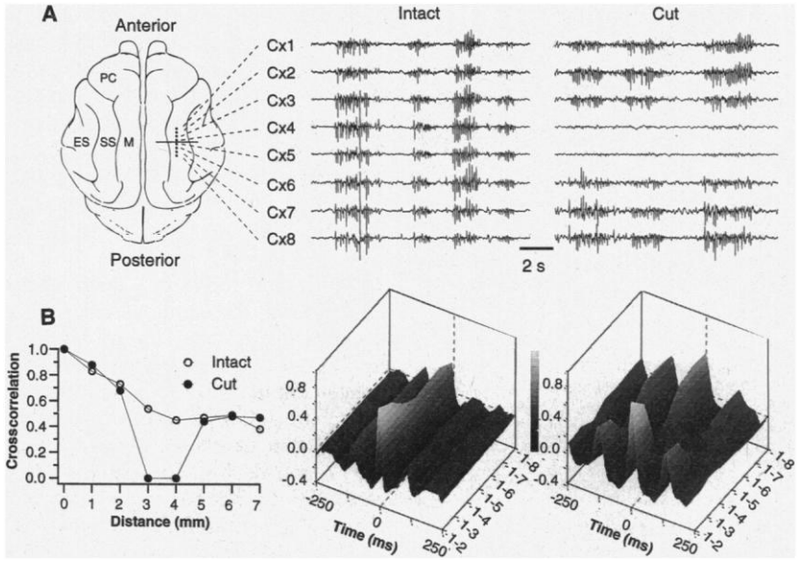

Fig. 4. Synchrony of spindle oscillations is not determined by intracortical connectivity. (**A**) Multisite recordings were taken from a 1-mm depth in the suprasylvian (SS) gyrus, with a similar electrode array (Cx1 to Cx8) as described in Fig. 1. Spontaneous spindle sequences occurred nearly simultaneously in control conditions (Intact). A 3-mm-deep coronal section (Cut) of the SS gyrus (horizontal line between electrodes Cx4 and Cx5 in the scheme), crossing laterally from the lateral aspect of the marginal gyrus (M) to the medial aspect of the ectosylvian gyrus (ES), did not disrupt simultaneity of oscillations. PC indicates postcruciate gyrus. (**B**) Synchronization was evaluated by calculating crosscorrelograms between electrode Cx1 and each of the others. Correlograms from 15 consecutive spindle sequences were averaged before and after the cut. The value of the averaged crosscorrelation at time zero was represented as a function of distance with respect to the first electrode. Averaged crosscorrelograms for each pair of electrodes were represented as surface plots for intact cortex (middle) and cortex after the cut (right). Correlation values were displayed with a gray scale ranging from −0.4 (black) to 1 (white; see grayscale bar). Secondary peaks around 120 ms indicate rhythmicity at 8 to 9 Hz.

REFERENCES AND NOTES

1. M. Steriade, E. G. Jones, R. R. Llinás, *Thalamic Oscillations and Signaling* (Wiley, New York, 1990); M. Steriade, D. A. McCormick, T. J. Sejnowski, *Science* **262**, 679 (1993).
2. R. S. Morison and D. L. Basset, *J. Neurophysiol.* **8**, 309 (1945). Electrophysiological experiments in vivo demonstrated that spindles could be generated in a surgically isolated patch containing the rostral pole of the RE nucleus [M. Steriade, L. Domich, G. Oakson, M. Deschênes, *ibid.* **57**, 260 (1987)] and that lesioning of the RE nucleus disrupted spindling in dorsal thalamic nuclei [M. Steriade, M. Deschênes, L. Domich, C. Mulle, *ibid.* **54**, 1473 (1985)]. In slices from the caudal thalamus, disconnection between RE cells and dorsal thalamus disrupted spontaneous oscillations in the RE nucleus [M. von Krosigk, T. Bal, D. A. McCormick, *Science* **261**, 361 (1993)], although RE cells generated intrinsic oscillations in the frequency range of spindling [T. Bal and D. A. McCormick, *J. Physiol. (London)* **468**, 669 (1993)]. Modeling studies have proposed a scenario to explain the absence of spindles in RE cells studied in vitro, based on the absence of neuromodulation in thalamic slices [A. Destexhe, D. Contreras, T. J. Sejnowski, M. Steriade, *Neuroreport* **5**, 2217 (1994)].
3. R. S. Morison and E. W. Dempsey, *Am. J. Physiol.* **138**, 297 (1943).
4. P. Andersen and S. A. Andersson, *Physiological Basis of the Alpha Rhythm* (Appleton-Century-Crofts, New York, 1968).
5. Thalamic spindles can be induced by cortical stimulation, even by stimulating the contralateral cortex to avoid backfiring of thalamocortical axons [M. Steriade, P. Wyzinski, V. Apostol, in *Corticothalamic Projections and Sensorimotor Activities*, T. L. Frigyesi, E. Rinvik, M. D. Yahr, Eds. (Raven, New York, 1972), pp. 221–272; D. Contreras and M. Steriade, *J. Physiol. (London)* **490**, 159 (1996)].
6. D. Contreras and M. Steriade, *J. Neurosci.* **15**, 604 (1995).
7. C. Koch, *Neuroscience* **23**, 399 (1987).
8. A. M. Sillito, H. E. Jones, G. L. Gerstein, D. C. West, *Nature* **369**, 479 (1994).
9. M. A. L. Nicolelis, R. C. S. Lin, D. J. Woodward, J. K. Chapin, *Proc. Natl. Acad. Sci. U.S.A.* **90**, 2212 (1993).
10. Propagation of spindle oscillations was observed in experiments on thalamic slices [U. Kim, T. Bal, D. A. McCormick, *J. Neurophysiol.* **74**, 1301 (1995)] and in computational models of thalamic slices [D. Golomb, X. J. Wang, J. Rinzel, *ibid.* **75**, 750 (1996); A. Destexhe, T. Bal, D. A. McCormick, T. J. Sejnowski, *ibid.* **76**, 2049 (1996)]. In the present in vivo experiments, we have only observed propagation of spindles in the thalamus after decortication as an exception. Spindle sequences occasionally showed synchrony even among widely spaced thalamic territories (Fig. 1, bottom; Fig. 2, decorticated spectra).
11. Power spectra were calculated according to W. H. Press, B. P. Flannery, S. A. Teukolsky, and W. T. Vetterling [*Numerical Recipes. The Art of Scientific Computing* (Cambridge Univ. Press, Cambridge, 1986)].
12. E. G. Jones, *The Thalamus* (Plenum, New York, 1985).
13. Intracellular recordings were obtained from the thalamus of decorticated animals with glass microelectrodes filled with 3 M potassium acetate and dc resistances of 35 to 45 megohms. Pipettes were held with two independent micromanipulators, and the distance between the tip was adjusted according to the point of penetration in the tissue. Cells recorded in the VL nucleus were reached by descending through the head of the caudate nucleus. The more posterior pipette penetrated through the exposed surface of the dorsal thalamus at stereotaxic coordinates corresponding to the lateral posterior (LP) nucleus. A total of eight stable couples was studied at distances of less than 1 to 2 mm and 12 couples at distances of 3 mm or more from six different animals. Stable recordings had resting membrane potentials more negative than −60 mV, overshooting action potentials and input resistances between 17 and 24 megohms. To ensure stability of intracellular recordings, we paralyzed the animals with galamine triethiodide (33 mg per kilogram of body weight, intravenously) and artificially ventilated them, with control of the end-tidal CO_2 concentration at around 3.7%. Further stability was obtained by performing cisternal drainage, bilateral pneumothorax, and hip suspension, and by filling the hole left by the decortication with a 4% agar solution. Body temperature was maintained at 37° to 38°C. A constant state of deep anesthesia was obtained by additional doses of barbiturate and continuous monitoring of the electroencephalogram (EEG) from the contralateral hemisphere. A high-impedance amplifier with active bridge circuitry was used to record and inject current in the cells. The signals were recorded on an eight-channel tape with bandpass of 0 to 9 kHz and digitized off-line at 10 kHz for analysis and display.
14. Intracellular recordings in barbiturate-anesthetized cats have shown that, during spindles, the GABA-containing RE cells generate rhythmic spike-bursts within the frequency range of spindling, superimposed on a slowly rising and decaying depolarizing envelope (*1*). Spike-bursts of RE cells, particularly those in the rostral pole and rostrolateral sector of the nucleus, impose rhythmic IPSPs onto a large number of TC cells through their divergent connections in the dorsal thalamus [M. Steriade, A. Parent, J. Hada, *J. Comp. Neurol.* **229**, 531 (1984)]. TC rebound bursts are generated at the offset of the IPSPs and transmitted back to RE cells, where they generate AMPA (α-amino-3-hydroxy-5-methyl-4-isoxazolepropionate)–kainate excitatory postsynaptic potentials (EPSPs) [T. Bal, M. von Krosigk, D. A. McCormick, *J. Physiol. (London)* **483**, 641 (1995)], and to neocortical cells, where glutamatergic EPSPs are at the basis of the spindle oscillations observable in the EEG [M. Steriade and M. Deschênes, in *Cellular Thalamic Mechanisms*, M. Bentivoglio and R. Spreafico, Eds. (Elsevier, Amsterdam, 1988), pp. 51–76].
15. I. Timofeev and M. Steriade, *J. Neurophysiol.*, in press.
16. C. Avendaño, E. Rausell, D. Perez-Aguilar, S. Isorna, *J. Comp. Neurol.* **278**, 1 (1988).
17. The possibility that corticocortical connections, other than those disrupted by the cut in the suprasylvian gyrus, might account for the preserved synchrony of spindles is remote, because the same type of suprasylvian transection succeeded in immediately disrupting the synchrony of an intracortically generated slow oscillation [F. Amzica and M. Steriade, *J. Neurosci.* **15**, 4658 (1995)].

18. We thank D. Drolet, P. Giguère, and G. Oakson for technical assistance. Supported by the Medical Research Council of Canada, Human Frontier Science Program, Fonds de la Recherche en Santé du Québec, and the Howard Hughes Medical Institute.

20 May 1996; accepted 23 August 1996

PIN: An Associated Protein Inhibitor of Neuronal Nitric Oxide Synthase

Samie R. Jaffrey and Solomon H. Snyder*

The neurotransmitter functions of nitric oxide are dependent on dynamic regulation of its biosynthetic enzyme, neuronal nitric oxide synthase (nNOS). By means of a yeast two-hybrid screen, a 10-kilodalton protein was identified that physically interacts with and inhibits the activity of nNOS. This inhibitor, designated PIN, appears to be one of the most conserved proteins in nature, showing 92 percent amino acid identity with the nematode and rat homologs. Binding of PIN destabilizes the nNOS dimer, a conformation necessary for activity. These results suggest that PIN may regulate numerous biological processes through its effects on nitric oxide synthase activity.

Nitric oxide (NO) is a major messenger molecule in the cardiovascular, immune, and nervous systems. In the brain, NO is responsible for the glutamate-linked enhancement of 3′,5′ cyclic guanosine monophosphate (cGMP) levels (*1*) and may be involved in apoptosis (*2*), synaptogenesis (*1, 3*), and neuronal development (*1*). Because NO cannot be stored in vesicles like other neurotransmitters, its release is regulated by the activity of the enzyme that makes it, NO synthase (NOS).

To search for associated proteins that might alter nNOS activity, we used the yeast two-hybrid system (*4, 5*). Yeast expressing a fusion protein consisting of amino acids 2 to 377 of nNOS and the Gal4 DNA-binding domain (BD) were transformed with a rat hippocampal cDNA library fused to the Gal4 activation domain (AD). Screening of ~3 × 10^6 clones resulted in the isolation of a cDNA that encodes a protein, designated PIN (protein inhibitor of nNOS), that interacts with nNOS (*6*). This interaction was specific because PIN binds to nNOS but not to distinct domains of another protein, the rapamycin and FKBP target (RAFT) (Fig. 1A). Expression of several truncated fragments of nNOS (*7*) as Gal4 BD fusions revealed that amino acids 163 to 245 of nNOS are sufficient for PIN binding in yeast (Fig. 1B). This region lies outside of the nNOS PDZ domain, a protein-binding module that may target nNOS to synaptic structures (*8, 9*), and it does not overlap with regions of nNOS previously implicated in binding to calmodulin or cofactors.

Northern (RNA) blot analysis with the PIN cDNA as a probe revealed an abundant 0.9-kb transcript present at highest levels in the testes, intermediate levels in the brain,

Departments of Neuroscience, Pharmacology and Molecular Sciences, and Psychiatry and Behavioral Sciences, Johns Hopkins University School of Medicine, 725 North Wolfe Street, Baltimore, MD 21205, USA.

*To whom correspondence should be addressed.